Revista Mexicana de Astronomía y Astrofísica, **60**, 293–304 (2024)

https://doi.org/10.22201/ia.01851101p.2024.60.02.07

SUPERNOVAE PHOTOMETRY AT OAUNI[1]

M. Espinoza[2] and A. Pereyra[3,2]

Received February 17 2024; accepted June 4 2024

ABSTRACT

We analyse photometric data of nine supernovae (SNe) in filters V, R and I obtained during observational campaigns at the OAUNI site in 2016, 2017 and 2023. The calibrated magnitudes of the observed SNe were compared with their respective light curves available in the literature to study their evolution after their maximum brightness. In some cases, the supernova color-color diagnostic diagram was used to determine our observation date and correctly locate our magnitudes on the light curves. For this purpose, the use of supernova light curve templates, as well as reference supernovae, was also helpful. This work allowed us to verify the feasibility of performing precision astronomical photometry at the OAUNI.

RESUMEN

Analizamos los datos fotométricos de nueve supernovas en los filtros V, R e I que se obtuvieron durante las campañas observacionales de OAUNI en 2016, 2017 y 2023. Para investigar la evolución posterior a su punto máximo de brillo, se compararon las magnitudes calibradas de las supernovas observadas con sus respectivas curvas de luz disponibles en la literatura. En algunos casos, se usó el diagrama de diagnóstico color-color de supernovas para determinar nuestras fechas de observación y ubicarlas correctamente en las curvas de luz. Para este propósito también fueron de ayuda la utilización de plantillas de curvas de luz de supernovas, así como supernovas de referencia. Este trabajo permitió verificar la factibilidad de realizar fotometría astronómica de precisión en el OAUNI.

Key Words: supernovae: general — techniques: photometric

1. INTRODUCTION

The Astronomical Observatory of the National University of Engineering (OAUNI in Spanish) began operations in 2015 (Pereyra et al. 2015). This facility is situated in Huancayo, 3300 meters above sea level, in the heart of the Peruvian Andes. One of the main scientific programs proposed was the supernovae photometric follow-up with several detections since then. This work presents the main SNe events observed at OAUNI site in the last years since 2016. Special care was taken for the photometric calibration process in order to contribute with useful data to the supernovae light curves of the analyzed events. Previous efforts of SNe observations in Perú include the detection of the famous SN 1987 by M. Ishitsuka and H. Trigoso (private communication) at the same site of these observations, and SN 2003gt (Carlos Reyes et al. 2013) observed at the southern Peruvian Andes.

In the following, we describe the observed SNe (§ 2), and the reduction process (§ 3), including the different methods used for the calibration data. The analysis and comparison of OAUNI data with template light curves, diagnostic color-color diagrams, and data available in the literature for each event is shown in § 4. Finally, our conclusions are drawn in § 5.

2. DETECTED OAUNI SUPERNOVAE EVENTS

The OAUNI SNe sample is indicated in Table 1 and Figure 1. A total of nine events were detected including four SNe Type Ia, four Type II, and one Type Ib. All the analyzed SNe are at a redshift lower than 0.04 (see Table 1). Below is listed the relevant information about each event.

[1]Observations obtained at the Astronomical Observatory of the National University of Engineering (OAUNI) in Huancayo, Perú.

[2]National University of Engineering, Lima, Perú.

[3]Geophysical Institute of Perú, Astronomy Area, Lima, Perú.

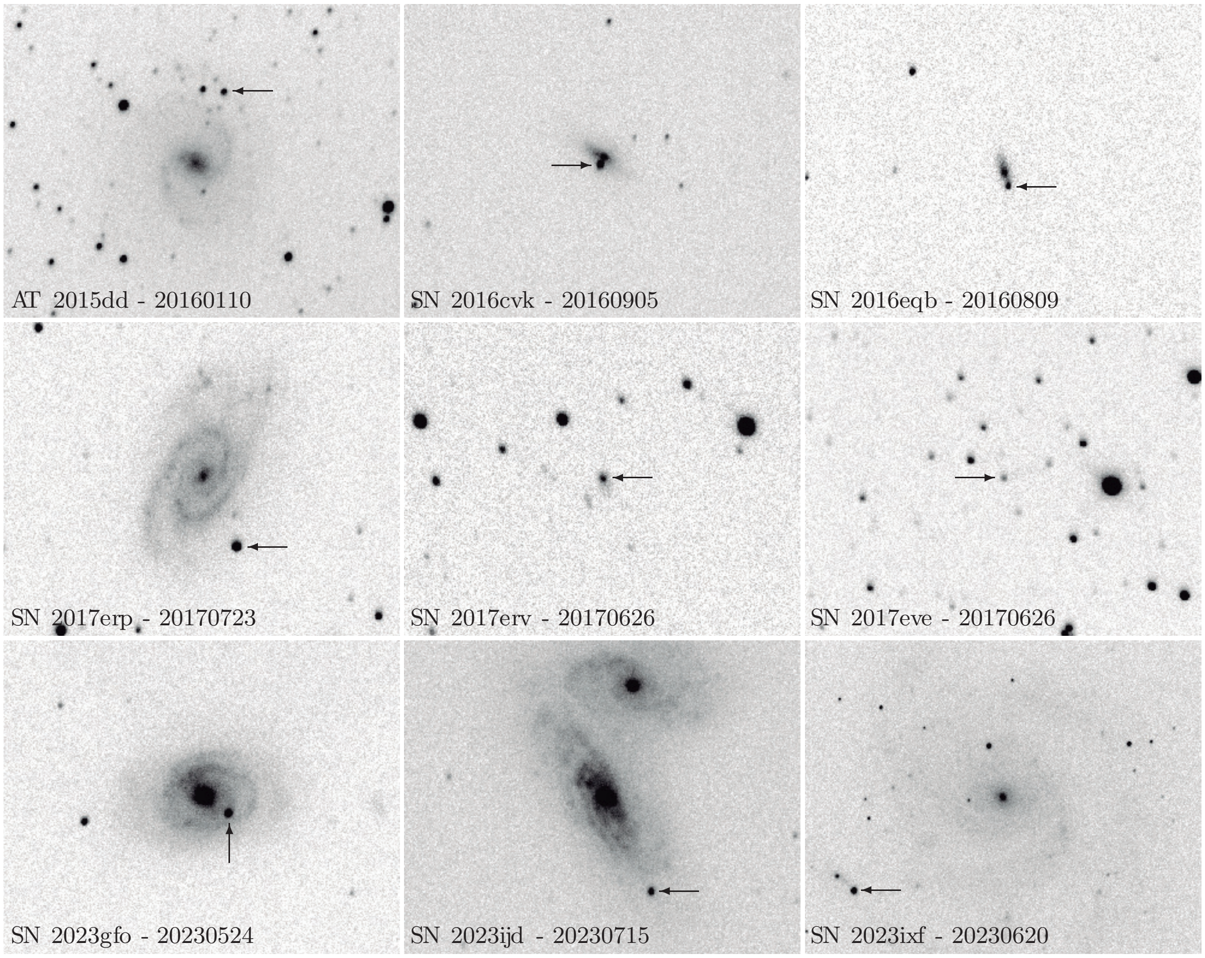

Fig. 1. OAUNI SNe sample in the R filter. Each frame indicates the observed SN (arrow) and the observation date. The individual FOV is $4.'1\times3.'2$, except for SN 2023ixf with $9.'6\times7.'7$. North is top and East is left.

2.1. *AT 2015dd*

On December 15, 2015, AT 2015dd was found in the center of the galaxy NGC 5483 ($z = 0.006$) by the MASTER-SAAO[4] (Gress et al. 2015). Using the SOAR telescope, three days later, it was identified as a Type Ib SN, and 2015-12-08 was determined to be the day of maximum brightness (Foley, Hounsell & Miller 2015).

2.2. *SN 2016cvk*

On June 12, 2016, the BOSS group[5] discovered SN 2016cvk. The SN was situated east of the host galaxy ESO 344-G 021 (z=0.010783, Parker 2016), and had a very low brightness of ≈17 mag in the V filter. With a behavior very similar to SN 2009ip, the *ASASSN* group[6] classified this SN as Type IIn. The PESSTO group (Parker 2016) further confirmed this classification.

2.3. *AT 2016eqb*

On August 1, 2016, the *ASASSN* group (Brimacombe et al. 2016) identified AT 2016eqb in the host galaxy 2MASX J23154564-0120135 (z=0.025308). KOSMOS[7] classified it as a Type Ia SN, with the day of maximum brightness being 2016-08-07 (Pan et al. 2016).

2.4. *SN 2017erp*

K. Itagaki discovered SN 2017erp on June 13, 2017 (Itagaki 2017). SALT[8] (Jha et al. 2017) classified it as an extremely young Type Ia SN, located in the arm of NGC 5861

[4]Mobile Astronomical System of Telescope-Robots at the South African Astronomical Observatory, a self-detection system.

[5]Backyard Observatory Supernova Search.

[6]All-Sky Automated Survey for SNe.

[7]The Cosmic Evolution Survey (COSMOS).

[8]The Southern African Large Telescope.

($z = 0.006174 \pm 0.000003$, Theureau et al. 2020). This SN was of special interest because of the relationship between its non-homogeneous composition and its light curve, as well as the peculiar reddening of its spectral lines in the near-ultraviolet range.

2.5. *AT 2017erv and AT 2017eve*

The *ASASSN* group found AT 2017erv on 2017-06-13 in AM 1904-844 (z=0.017035). A few days later, on June 19, 2017, AT 2017eve was also found on the same images in GALEXASC J184352.21-562927.7 (z=0.031, Nicholls, Brimacombe & Cacella 2017). On June 20, 2017, Uddin et al. (2017) categorized both SNe as Type Ia SNe, with a phase from maximum brightness of −2 days for AT 2017erv and +2 days for AT 2017eve.

2.6. *SN 2023gfo*

On 2023-04-19, SN 2023gfo was detected in NGC 4995 (z=0.0058) by the ATLAS[9] system. Additionally, the same field was observed four days prior to this detection, but no sign of the SN was found. According to Moore et al. (2023), this event would suggest that the SN was in its growth phase. Lick Observatory classified it as a SN Type IIP with a spectrum remarkably similar to SN 1999gi (Fulton et al. 2023b).

2.7. *SN 2023ijd*

The *ASASSN* group found SN 2023ijd in NGC 4568 ($z = 0.007446$, Stanek 2023) on 2023-05-14. It was classified as a Type II SN (Perley 2023).

2.8. *SN 2023ixf*

SN 2023ixf was classified as a Type II SN in its early stages of life (Perley & Gal-Yam 2023) after K. Itagaki discovered it on May 19, 2023, in M101 (z=0.000804, Itagaki 2023). Over the past few decades, SN 2023ixf has been considered the nearest Type II SN. Subsequent reports of earlier sightings, following the discovery, helped narrow down the explosion date (Fulton et al. 2023a; Filippenko, Zheng & Yang 2003) to a 20-hour window between May 18 and 19. SN 2023ixf was later reclassified as Type II-L (Bianciardi et al. 2023).

3. OBSERVATIONS, REDUCTIONS AND CALIBRATIONS

All observations mentioned here were collected using the OAUNI telescope (Pereyra et al. 2015) during the 2016, 2017, and 2023 observation campaigns. These observational runs typically take place in the months of May through September. In only one instance (AT 2015dd), a single observation was made in January. The OAUNI telescope has a Cassegrain type optical tube with Ritchey-Chrétien design and a primary mirror with a diameter of 0.51 m and f/8.2. A front-illuminated CCD STXL-6303E with 3072×2048 pixels^2 and 9μm/pixel served as the detector. A field-of-view of $\approx 23' \times 15'$ and a plate scale of 0.45″/pixel are produced by this detector and the optical system's focal ratio. For the scientific objects, multicolor photometry was made possible via a *UBVRI* filter wheel. The record of observations made during the campaigns is displayed in Table 2. Column 1 shows the name of the SN, Column 2 presents the local observation date, Column 3 indicates the filters used, Column 4 displays the number of images obtained in each filter, and Column 5 shows the total integration time for each case. Column 6 presents the mean air mass during each sequence. In total, data from nine SNe are presented, with three different SNe observed each year. The individual integration time for one measurement is 20 seconds, and the total time for stacking images (N×20s) ranges from 600 to 1400 seconds.

With standard corrections for dark current and flat field, we used IRAF[10] for image reduction. Aperture photometry was extensively used with a typical instrumental magnitude error of tens of milimagnitude for the magnitude range of our sample (typically, between 11.3 to 17.1 mag). The first step in the calibration process was to find stars in each stellar field that matched both our images and the UCAC4 photometric catalog (Zacharias et al. 2013). These stars, listed in Table 3, were then used as comparison stars for every SN analyzed. We utilized two methods to determine the corrected value of the SN brightness using this data. The first method (m_1), involving equations 1, 2, and 3, was used to represent the transformation of the instrumental magnitudes (v, i, and r) to the calibrated magnitudes (V, I, and R) by obtaining a single zero point (v_0, i_0, and r_0). This method is useful when only one filter is available for measurements and was used for all the objects in our sample.

$$V = v_0 + v, \tag{1}$$

$$R = r_0 + r, \tag{2}$$

$$I = i_0 + i. \tag{3}$$

Using the transformation equations, the second method (m_2) involves the zero points (v_0, r_0, and i_0), the linear dependence (v_1, r_1, and i_1), and the

[9]Asteroid Terrestrial-Impact Last Alert System.

[10]Image Reduction and Analysis Facility hosted by the National Optical Astronomy Observatories in Tucson, Arizona.

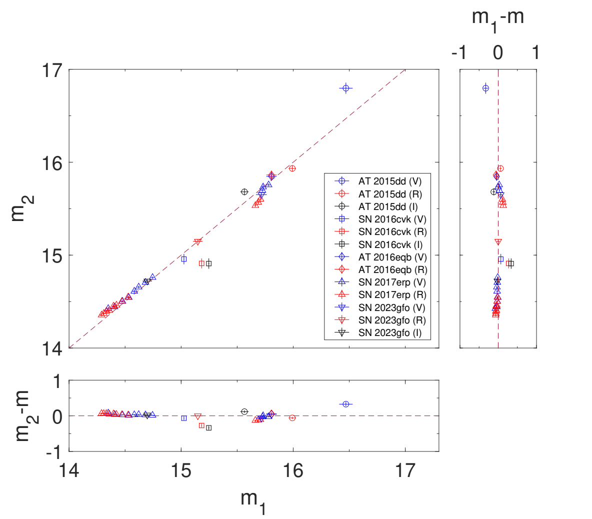

Fig. 2. Point-to-point correlation between m_1 and m_2 calibration methods for OAUNI SNe sample. Instrumental magnitudes in the V (blue dots), R (red dots) and I filters (black dots) are shown with different symbols for each supernova. The residuals for each calibration with respect to the perfect positive correlation (dashed line) are indicated below and on the right. The color figure can be viewed online.

coefficients (v_2, r_2, and i_2) for the color terms ($v-r$ or $v-i$) of the objects under consideration. The equations 4, 5, and 6 illustrate these transformations. This calibration method is more robust, but multicolor photometry is necessary for its applicability. It was used on five of the sample's objects.

$$V = v_0 + v_1 \times v + v_2 \times (v - r), \tag{4}$$

$$R = r_0 + r_1 \times r + r_2 \times (v - r), \tag{5}$$

$$I = i_0 + i_1 \times i + i_2 \times (v - i). \tag{6}$$

Our findings for the calibrations of the SNe magnitude of our sample, m_1 (Column 7) and m_2 (Column 8), are displayed in Table 2.

4. ANALYSES

Figure 2 displays m_1 and m_2 for any scenario in which both calibrations are provided for the same object so that the two calibration techniques can be compared. With the exception of 2016cvk, all examples have a high point-to-point correlation, and the typical residual between m_1 and m_2 is 0.096 ± 0.064 mag. When two calibrations are available, we will utilize m_2 for the analyses in the following; in other circumstances, we will use m_1.

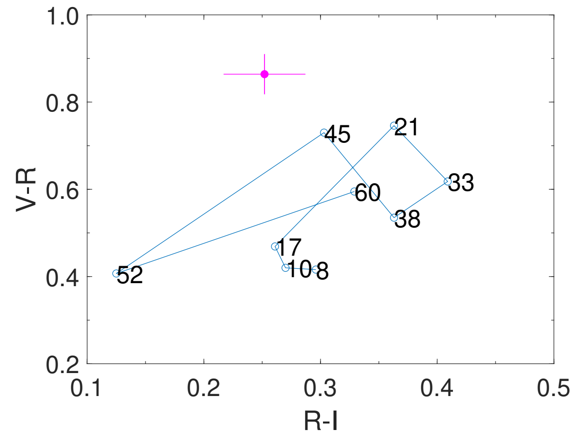

Fig. 3. $V-R$ vs. $R-I$ color diagram of Type Ib SN with $z = 0$ (blue line), adapted from Poznanski et al. (2002). Numbers indicate days after maximum light. OAUNI colors for AT 2015dd using the m_2 calibration are also indicated (magenta dot). The color figure can be viewed online.

4.1. *AT 2015dd*

When a SN reaches its maximum brightness, color-color diagnostic diagrams can be used to confirm how old it is (Poznanski et al. 2002). Based on the Type Ib SN classification of AT 2015dd and the near-zero redshift of the host galaxy (see to Table 1), Figure 3 illustrates the temporal behavior of a well-studied Type Ib SN at various stages of its life for $z = 0$. Using the m_2 calibration (Table 2), we computed the colors $V-R$ and $R-I$ for AT 2015dd. The values $V - R = 0.864 \pm 0.047$ and $R - I = 0.252 \pm 0.035$ are also displayed in Figure 3. The location of AT 2015dd on the diagram indicates a period of 20-40 days after the maximum of brightness, although it is not sufficient to explicitly validate the age of the supernova. Nevertheless, our observations are ≈32 days after the maximum, taking into account the day of the explosion on 2015-12-08 (Foley, Hounsell & Miller 2015).

4.2. *2016cvk*

Based on the information found in Table 2, we calculated the m_2 colors for SN 2016cvk, which are $V - R$=0.045 ± 0.004 and $R - I$=0.002 ± 0.005 on the Type IIn SN's $z = 0$ diagnostic diagram (refer to Figure 4). This SN 2016cvk is located almost exactly on the line that the diagram's days 3 through 13 encompass. It implies that when OAUNI observed this SN, it was still very young. On the other hand, we used a template (Nugent, Kim & Perlmutter 2002), literature data (see Table 4), and OAUNI m_2 data

TABLE 1

OAUNI SUPERNOVAE SAMPLE

SN	Other name	Type	RA (2000)	DEC (2000)	Discovery date (UT)	Host galaxy	z[a]
AT 2015dd	PSN J141[b]	Ib	14:10:23.42	-43:18:43.70	2015-12-15	NGC 5483	0.005921
SN 2016cvk	ASASSN-16jt	IIn-pec	22:19:49.43	-40:40:05.50	2016-06-12	ESO 344-G21	0.010842
AT 2016eqb	ASASSN-16hz	Ia	23:15:45.48	-01:20:22.73	2016-08-01	2MASX[c]	0.02531(15)
SN 2017erp		Ia	15:09:14.90	-11:20:03.00	2017-06-13	NGC 5861	0.006303
AT 2017erv	ASASSN-17ho	Ia	19:18:47.10	-84:41:50.03	2017-06-13	AM 1904-844	0.017035
AT 2017eve	ASASSN-17hq	Ia	18:43:53.51	-56:29:29.04	2017-06-19	GALEXASC[d]	0.031
SN 2023gfo		IIP	13:09:39.68	-07:50:11.75	2023-04-20	NGC 4995	0.005834
SN 2023ijd	ASASSN-23du	II	12:36:32.47	+11:13:19.71	2023-05-14	NGC 4568	0.00744(10)
SN 2023ixf		IIL	14:03:38.56	+54:18:41.94	2023-05-19	M101	0.000811(16)

[a] Of host galaxy from SIMBAD, except for AT 2016erv (Nicholls, Brimacombe & Cacella 2017) and AT 2017eve (Uddin et al. 2017).
[b] PSN J14102342-4318437.
[c] 2MASX J23154564-0120135.
[d] GALEXASC J184352.21-562927.7.

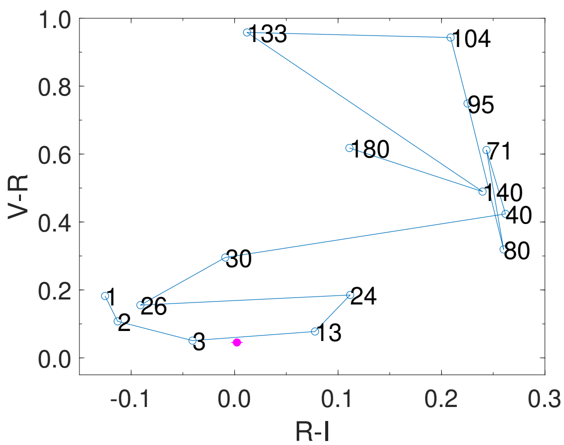

Fig. 4. $V - R$ vs. $R - I$ color diagram of Type IIn SN with $z = 0$ (blue line, adapted from Poznanski et al. 2002). Numbers indicate days after maximum light. OAUNI colors for SN 2016cvk using m_2 calibration are also indicated (magenta dot). The color figure can be viewed online.

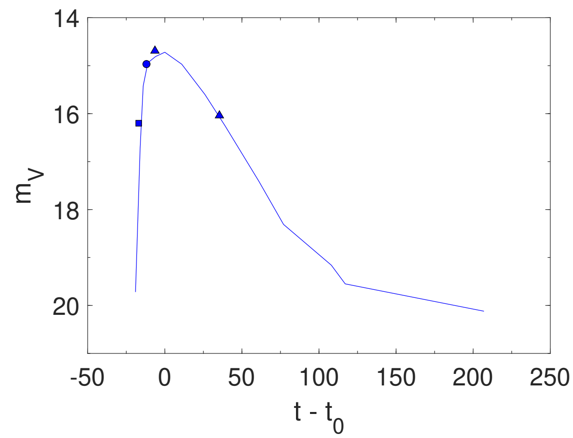

Fig. 5. SN 2016cvk light curve in the V filter. Template light curve for Type IIn SN with $z = 0$ (blue line, Nugent, Kim & Perlmutter 2002) with *ASASSN* data (blue square, Brimacombe et al. 2016), Kato's data (blue triangle, `http://ooruri.kusastro.kyoto-u.ac.jp/mailarchive/vsnet-recent-sn/6612`) and OAUNI m_2 data (blue dot, Table 2). Time offset is t_0 = 2457648.5 days. The color figure can be viewed online.

(see Table 2) to generate the light curve in the V filter for this SN. To determine whether the brightness of this SN behaves similarly to the average brightness of SNe of the same type, the Nugent's template is shown. In order to compare the data, we must fit all of the data to the same reference system because Nugent's template plots the peak of brightness in the B filter of the time coordinate. First, we use equation 7 to convert the numbers at the template's peak to a polynomial.

$$m(t) = \sum_{i=0}^{6} m_i \times (t - t_0)^i. \tag{7}$$

Using data from the SN close to the peak, we modify m_0 and t_0 in this polynomial to determine the values that present the least residual. We divide the duration of the data by 1+z to subtract the z contribution of the host galaxy (see Table 1) before substituting this data. In order to modify the template to fit the displayed data, we acquired the final vector (t_0; m_0) after changing the SN data (see Table 5). Since the maximum brightness date is unknown, we set the beginning t_0 value for the fitting using the information provided by the diagnostic diagram (Figure 4). The ultimate outcome of the development of the light curve, where the data follows the template, is shown in Figure 5. The diagnostic diagram places this event around day 10 after the peak; however, the OAUNI data is situated around day ≈ -12 before the peak.

TABLE 2

OAUNI SUPERNOVAE OBSERVATION LOG

SN (1)	Date (UTC) (2)	Filter (3)	N (4)	IT (s) (5)	X (6)	m1 (7)	m2 (8)
AT 2015dd	2016/01/10.385	V	30	600	1.467	16.470 ± 0.060	16.797 ± 0.060
	2016/01/10.396	R	30	600	1.402	15.992 ± 0.033	15.933 ± 0.033
	2016/01/10.410	I	30	600	1.336	15.565 ± 0.037	15.681 ± 0.037
SN 2016cvk	2016/09/05.084	V	90	1800	1.375	15.025 ± 0.079	14.957 ± 0.052
	2016/09/05.099	R	90	1800	1.305	15.183 ± 0.076	14.911 ± 0.050
	2016/09/05.113	I	90	1800	1.250	15.247 ± 0.079	14.909 ± 0.065
AT 2016eqb	2016/08/09.405	V	45	900	1.310	15.806 ± 0.046	15.847 ± 0.046
	2016/08/09.390	R	45	900	1.243	15.806 ± 0.046	15.863 ± 0.046
SN 2017erp	2017/07/23.087	V	45	900	1.064	14.349 ± 0.014	14.424 ± 0.019
	2017/07/23.055	R	45	900	1.167	14.289 ± 0.015	14.355 ± 0.022
	2017/07/24.066	V	45	900	1.156	14.406 ± 0.011	14.442 ± 0.018
	2017/07/24.050	R	45	900	1.100	14.309 ± 0.015	14.372 ± 0.019
	2017/07/25.103	V	45	900	1.195	14.476 ± 0.011	14.502 ± 0.016
	2017/07/25.087	R	45	900	1.280	14.332 ± 0.016	14.395 ± 0.022
	2017/07/26.200	V	45	900	2.756	14.533 ± 0.013	14.544 ± 0.017
	2017/07/26.186	R	45	900	3.614	14.359 ± 0.014	14.405 ± 0.016
	2017/07/27.059	V	45	900	1.041	14.581 ± 0.018	14.611 ± 0.020
	2017/07/27.034	R	45	900	1.104	14.396 ± 0.017	14.450 ± 0.013
	2017/07/28.042	V	45	900	1.035	14.621 ± 0.014	14.656 ± 0.016
	2017/07/28.027	R	45	900	1.065	14.423 ± 0.014	14.461 ± 0.016
	2017/07/29.053	V	45	900	1.064	14.682 ± 0.012	14.706 ± 0.016
	2017/07/29.039	R	45	900	1.105	14.471 ± 0.012	14.501 ± 0.015
	2017/07/30.044	V	45	900	1.049	14.745 ± 0.011	14.759 ± 0.016
	2017/07/30.029	R	45	900	1.085	14.527 ± 0.012	14.548 ± 0.015
	2017/08/21.041	V	45	900	1.255	15.725 ± 0.014	15.695 ± 0.013
	2017/08/21.025	R	45	900	1.362	15.662 ± 0.016	15.532 ± 0.010
	2017/08/22.064	V	20	400	1.350	15.731 ± 0.026	15.733 ± 0.016
	2017/08/22.036	R	15	300	1.617	15.680 ± 0.019	15.568 ± 0.014
	2017/08/23.090	V	60	1200	1.747	15.780 ± 0.016	15.755 ± 0.018
	2017/08/23.070	R	60	1200	2.145	15.707 ± 0.026	15.601 ± 0.010
AT 2017erv	2017/06/26.354	R	45	900	3.535	15.423 ± 0.030	
	2017/06/27.085	R	45	900	3.907	15.372 ± 0.018	
AT 2017eve	2017/06/26.386	R	45	900	2.138	17.010 ± 0.032	
	2017/06/27.156	R	45	900	1.503	17.077 ± 0.033	
	2017/06/28.158	R	90	1800	1.485	17.145 ± 0.028	
SN 2023gfo	2023/05/24.228	V	45	900	1.637	15.716 ± 0.025	15.651 ± 0.048
	2023/05/24.242	R	45	900	1.866	15.149 ± 0.022	15.149 ± 0.042
	2023/05/24.212	I	45	900	1.457	14.698 ± 0.021	14.721 ± 0.042
	2023/06/20.079	R	60	1200	1.108	15.417 ± 0.025	
	2023/06/21.091	R	80	1600	1.162	15.507 ± 0.025	
	2023/07/14.022	R	70	1400	1.144	15.720 ± 0.025	
	2023/07/15.045	R	70	1400	1.275	15.616 ± 0.025	
	2023/07/16.084	R	70	1400	1.663	15.592 ± 0.023	
	2023/07/17.079	R	70	1400	1.633	15.680 ± 0.025	
	2023/07/18.105	R	70	1400	2.153	15.431 ± 0.023	
	2023/07/20.102	R	70	1400	2.231	15.604 ± 0.026	
	2023/07/21.107	R	70	1400	2.465	15.540 ± 0.024	
	2023/08/16.057	R	70	1400	3.761	16.131 ± 0.032	
	2023/08/17.039	R	90	1400	2.801	16.636 ± 0.038	
	2023/08/18.038	R	90	1400	2.903	16.706 ± 0.038	
	2023/08/19.038	R	90	1400	2.768	16.391 ± 0.034	
SN 2023ijd	2023/07/15.070	R	70	1400	2.554	15.571 ± 0.022	
	2023/07/16.054	R	70	1400	2.174	15.613 ± 0.018	
	2023/07/17.050	R	70	1400	2.135	15.557 ± 0.018	
	2023/07/18.071	R	70	1400	2.908	15.621 ± 0.022	
	2023/07/20.070	R	70	1400	3.200	15.568 ± 0.013	
	2023/07/21.079	R	70	1400	4.045	15.591 ± 0.018	
SN 2023ixf	2023/06/20.021	R	54	1080	2.499	11.285 ± 0.025	
	2023/06/21.022	R	50	1000	2.483	11.301 ± 0.023	
	2023/07/14.050	R	53	1060	2.804	11.635 ± 0.024	
	2023/07/16.025	R	50	1000	2.615	11.606 ± 0.024	
	2023/07/17.018	R	50	1000	2.585	11.600 ± 0.029	
	2023/07/18.031	R	50	1000	2.715	11.690 ± 0.023	
	2023/07/20.038	R	53	1060	2.856	11.704 ± 0.026	
	2023/07/21.052	R	50	1000	3.131	11.714 ± 0.027	

4.3. *AT 2016eqb*

Since the maximum brightness date for AT 2016eqb is known (Pan et al. 2016), we have plotted it alongside the OAUNI m_2 data (see Table 2) and the available literature data (see Table 4) using the least residual method to determine m_0 only and fit the type Ia SN Nugent's template in the V filter. Since the host galaxy's z value is known in this instance as well (see Table 1), we used all of the data points that are near the peak to calculate the value of m_0. Nugent's template in the V filter with the appropriate t_0 and m_0 adjustments, as well as the OAUNI photometry of AT 2016eqb, are displayed in Figure 6 (see Table 5).

4.4. *2017erp*

We utilized values close to the peak of the light curves (15 days before and after the maximum) in both filters (V and R) to fit the type Ia SN Nugent's

TABLE 3

UCAC4 COMPARISON STARS

UCAC4 name	V_{cat} (mag) (1)	R_{cat} (mag) (2)	I_{cat} (mag) (3)
		AT 2015dd	
235-072564	11.356	10.968	10.607
235-072546	12.711	12.394	12.108
234-070894	9.800	9.879	9.879
234-070931	10.706	10.353	9.965
234-070956	12.923	12.591	12.292
		SN 2016cvk	
247-183586	12.291	12.176	12.060
247-183587	15.491	15.333	15.205
247-183594	14.920	14.771	14.651
247-183606	14.646	14.477	14.352
247-183607	13.416	13.317	13.222
247-183608	14.249	14.099	13.966
248-191420	12.131	11.962	11.834
248-191421	15.182	15.036	14.954
		AT 2016eqb	
444-131450	16.501	15.924	-
444-131442	15.745	15.506	-
445-136436	16.153	16.061	-
445-136441	16.506	16.386	-
445-136458	15.839	15.539	-
445-136465	16.083	15.858	-
		SN 2017erp	
394-058196	14.691	14.464	-
394-058202	14.800	14.535	-
394-058177	14.867	14.717	-
393-061368	15.085	14.916	-
394-058204	15.196	14.986	-
394-058168	15.204	14.870	-
		AT 2017erv	
027-009815	-	12.024	-
027-009769	-	12.309	-
027-009780	-	12.704	-
027-009785	-	12.884	-
027-009751	-	12.937	-
027-009784	-	12.985	-
027-009787	-	13.197	-
027-009792	-	13.255	-
027-009754	-	13.413	-
027-009747	-	13.431	-
027-009800	-	13.443	-
027-009768	-	13.487	-
027-009794	-	13.543	-
027-009807	-	13.547	-
027-009809	-	13.754	-
027-009755	-	13.775	-
		AT 2017eve	
168-205741	-	12.147	-
168-205790	-	12.191	-
168-205740	-	12.395	-
168-205715	-	12.493	-
168-205795	-	12.778	-
168-205776	-	13.051	-
168-205727	-	13.226	-
168-205789	-	13.628	-
168-205806	-	13.716	-
169-196343	-	13.748	-
168-205754	-	13.781	-
169-196291	-	13.947	-
168-205770	-	13.952	-
168-205798	-	13.996	-
169-196333	-	14.000	-
		SN 2023gfo	
412-054666	14.292	14.114	14.018
412-054667	14.279	14.121	14.030
412-054681	15.068	14.674	14.433
411-055301	15.112	14.930	14.793
411-055298	14.656	14.203	13.907
411-055299	15.053	14.781	14.604

TABLE 3. CONTINUED

UCAC4 name	V_{cat} (mag) (1)	R_{cat} (mag) (2)	I_{cat} (mag) (3)
		SN 2023ijd	
506-053220	-	15.925	-
506-053224	-	15.901	-
506-054413	-	16.161	-
506-054416	-	15.760	-
506-054417	-	15.790	-
506-054418	-	16.008	-
		SN 2023ixf	
723-053563	-	15.400	-
723-053565	-	14.719	-
723-053569	-	14.582	-
722-053112	-	15.410	-
722-053102	-	14.245	-
722-053103	-	15.298	-

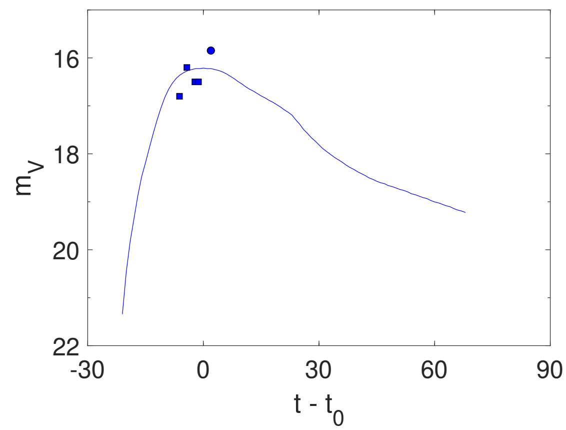

Fig. 6. AT 2016eqb light curve in the V filter. Template light curve for Type Ia SN with $z = 0$ (blue line, Nugent, Kim & Perlmutter 2002) with *ASASSN* data (blue squares, Brimacombe et al. 2016) and OAUNI m_2 data (blue dot, Table 2). Time offset is $t_0 = 2457607.5$ days. The color figure can be viewed online.

template because of the large amount of available literature data. The least residual approach was used to compute m_0, similar to the last supernova, since the date of the maximum brightness is known ($t_0 =$ 2457934.9 JD, Brown et al. 2016). We got distinct values of m_0 (see Table 5) for each filter, accounting for z from its host galaxy (see Table 1). Using the OAUNI m_2 data (see Table 2) and the available literature data for SN 2017erp (Brown et al. 2016), Figures 7 and 8 display the light curves in the V and R filters with their corresponding templates. Both charts demonstrate how well the OAUNI data match the data from UVOT, LCO, and AZT[11]. Even while the V filter's light curve up to day ≈30 follows the template's trend, as the days pass, the discrepancy becomes larger. The R filter's light curve, on the

[11]Shamakhi Astrophysical Observatory.

DOI: https://doi.org/10.22201/ia.01851101p.2024.60.02.07

TABLE 4

AVAILABLE LITERATURE LIGHT CURVE DATA

SN	Date (UT)	G	V	R	Reference
SN 2016cvk	2016-08-31.09	-	16.2	-	(a)
	2016-09-10.60	-	14.69	-	(b)
	2016-10-22.42	-	16.04	-	(b)
AT 2016eqb	2016-08-01.35	-	16.8	-	(a)
	2016-08-03.27	-	16.2	-	(a)
	2016-08-05.31	-	16.5	-	(a)
	2016-08-06.18	-	16.5	-	(a)
AT 2017erv	2017-06-11.23	-	16.6	-	(c)
	2017-06-13.31	-	16.2	-	(c)
	2017-06-13.38	-	16.1	-	(c)
	2017-06-19.25	-	15.8	-	(c)
	2017-07-13.04	16.67	-	-	(d)
	2017-07-13.08	16.66	-	-	(d)
	2017-08-10.08	17.75	-	-	(d)
	2017-08-10.29	17.77	-	-	(d)
	2017-09-14.33	18.74	-	-	(d)
	2017-10-19.25	19.41	-	-	(d)
	2017-10-19.29	19.43	-	-	(d)
	2017-11-09.96	19.81	-	-	(d)
	2017-11-10.04	19.86	-	-	(d)
	2017-12-19.67	20.22	-	-	(d)
AT 2017eve	2017-06-11.18	-	16.6	-	(c)
	2017-06-13.26	-	16.9	-	(c)
	2017-06-19.14	-	16.5	-	(c)
	2017-08-01.29	18.45	-	-	(e)
	2017-08-01.54	18.41	-	-	(e)
	2017-08-01.63	18.43	-	-	(e)
	2017-08-01.88	18.47	-	-	(e)
	2017-08-01.88	18.47	-	-	(e)
	2017-08-02.13	18.48	-	-	(e)
	2017-08-02.29	18.49	-	-	(e)
	2017-08-02.38	18.47	-	-	(e)
	2017-08-02.54	18.48	-	-	(e)
	2017-08-02.63	18.48	-	-	(e)
	2017-08-02.79	18.50	-	-	(e)
	2017-08-02.88	18.51	-	-	(e)
	2017-08-03.04	18.50	-	-	(e)
	2017-08-03.13	18.50	-	-	(e)
	2017-08-03.29	18.55	-	-	(e)
	2017-08-03.63	18.54	-	-	(e)
	2017-08-03.88	18.51	-	-	(e)
	2017-08-04.13	18.53	-	-	(e)
	2017-08-05.29	18.58	-	-	(e)
	2017-08-05.38	18.63	-	-	(e)
	2017-08-05.54	18.58	-	-	(e)
	2017-08-05.63	18.58	-	-	(e)
	2017-08-05.79	18.61	-	-	(e)
	2017-08-05.88	18.60	-	-	(e)
	2017-08-06.04	18.64	-	-	(e)
	2017-08-06.29	18.62	-	-	(e)
	2017-08-06.38	18.61	-	-	(e)
	2017-08-06.54	18.58	-	-	(e)
	2017-08-06.79	18.62	-	-	(e)
	2017-09-20.54	19.88	-	-	(e)
	2017-10-25.08	20.59	-	-	(e)
SN 2023ijd	2023-07-01.21	-	-	15.649±0.031	(f)
	2023-06-29.17	-	-	15.661±0.030	(f)
	2023-06-21.21	-	-	15.701±0.034	(f)
	2023-06-14.17	-	-	15.689±0.041	(f)
	2023-06-06.29	-	-	15.667±0.026	(f)
	2023-06-04.21	-	-	15.601±0.029	(f)
	2023-06-02.21	-	-	15.606±0.031	(f)
	2023-05-17.21	-	-	15.796±0.033	(f)
	2023-05-15.29	-	-	16.121±0.039	(f)

[a] Brimacombe et al. (2016)
[b] http://ooruri.kusastro.kyoto-u.ac.jp/mailarchive/vsnet-recent-sn/6612.
[c] Nicholls, Brimacombe & Cacella (2017)
[d] http://gsaweb.ast.cam.ac.uk/alerts/alert/Gaia17bto/.
[e] http://gsaweb.ast.cam.ac.uk/alerts/alert/Gaia17byi/.
[f] https://lasair-ztf.lsst.ac.uk/objects/ZTF23aajrmfh/.

TABLE 5

OAUNI SUPERNOVAE PARAMETERS

SN	Filter	Peak date (JD)	m_0 (mag)	Residual (mag) (x10^{-4})
AT 2015dd	-	2457374.5	-	-
SN 2016cvk	R	2457648.5	14.7197	1.0569
AT 2016eqb	V	2457607.5	16.2130	2.1325
SN 2017erp	R	2457934.9	13.5922	3.0811
	V	2457934.9	13.4813	2.6995
AT 2017erv	R	2457926.5	15.2615	2.8972
AT 2017eve	R	2457922.5	16.6213	3.5673
SN 2023gfo	R	2460049.7	15.1622*	2.8806
SN 2023ijd	R	2460088.9	15.6157*	2.7022
SN 2023ixf	R	2460094.0	-	-

*SN 2004et was used as a template

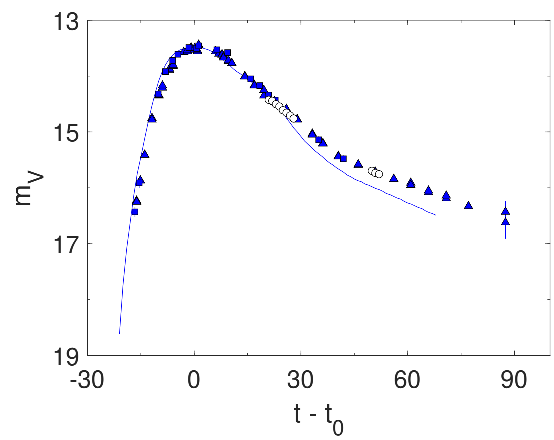

Fig. 7. SN 2017erp light curve in the V filter. Template light curve for Type Ia SN with $z = 0$ (blue line, Nugent, Kim & Perlmutter 2002) with UVOT data (blue squares, Brown et al. 2016), LCO data (blue triangles, Brown et al. 2016) and OAUNI m_2 data (white dots, Table 2). Time offset is $t_0 = 2457934.9$ days. The color figure can be viewed online.

other hand, traces the trend both before and after the maximum brightness.

4.5. *AT 2017erv*

The AT 2017erv light curve in V and R filters, together with the type Ia SN Nugent's templates, is displayed in Figure 9 using OAUNI m_1 data (see Table 2) and the available literature data (see Table 4). In order to fit template in filter R, we used the host galaxy redshift information (see Table 1) and the date of the maximum brightness (Uddin et al. 2017). Since OAUNI data are in the R filter, the template for this filter was used as a reference to plot the template in the V filter. This is a feature of Nugent's template, as each template was created using a correlation filter-to-filter. To do this, we found m_0 with the least residual by substituting OAUNI m_1 data in the polynomial fit for the template in filter R (see Table 5). Next, we used Nugent's SN Ia template light curve to compare the OAUNI findings in the R filter (Table 2) with the values found by $GAIA$ and $ASASSN$ for the V and G filters, since this SN was categorized as a Type Ia (Uddin et al. 2017). The outcome of fitting Nugent's template to OAUNI R filter data is displayed in Figure 9. Furthermore, we can see that, in contrast to the template in the V fil-

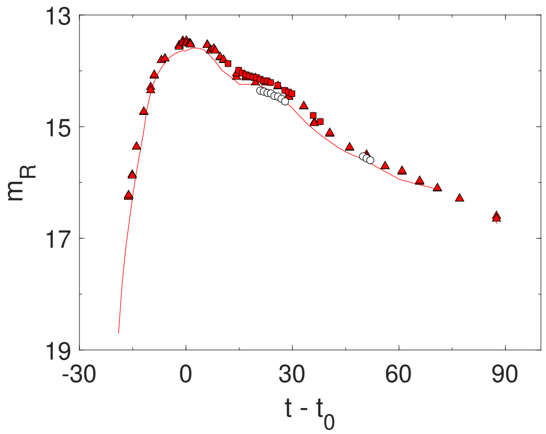

Fig. 8. SN 2017erp light curve in R filter. Template light curve for Type Ia SN with $z = 0$ (red line, Nugent, Kim & Perlmutter 2002) with AZT data (red squares, Brown et al. 2016), LCO data (red triangles, Brown et al. 2016) and OAUNI m_2 data (white dots, Table 2). Time offset is $t_0 = 2457934.9$ days. The color figure can be viewed online.

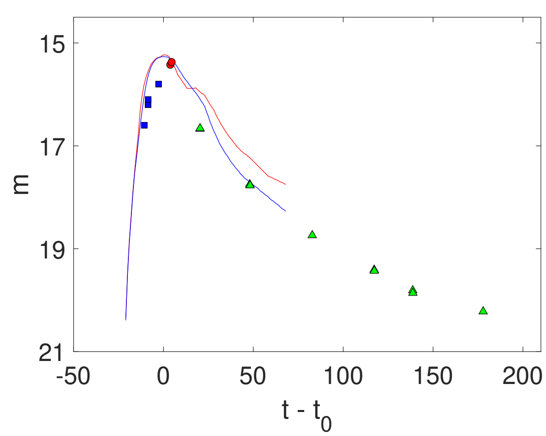

Fig. 9. AT 2017erv light curve. Template light curve for Type Ia SN in V (blue line) and R (red line) filters with $z = 0$ (Nugent, Kim & Perlmutter 2002), with *ASASSN* data (V filter, blue squares, Nicholls, Brimacombe & Cacella 2017), GAIA data (G filter, green triangles, `http://gsaweb.ast.cam.ac.uk/alerts/alert/Gaia17bto/`) and OAUNI data (R filter, red dots, Table 2). Time offset is $t_0 = 2457926.5$ days. The color figure can be viewed online.

ter, the *ASASSN* data exhibit a continuous rise in brightness before the peak, whereas the *GAIA* data have a faster fall rate.

4.6. *AT 2017eve*

We have used Nugent's templates in the R and V filters, like for the previous SN. We employed OAUNI

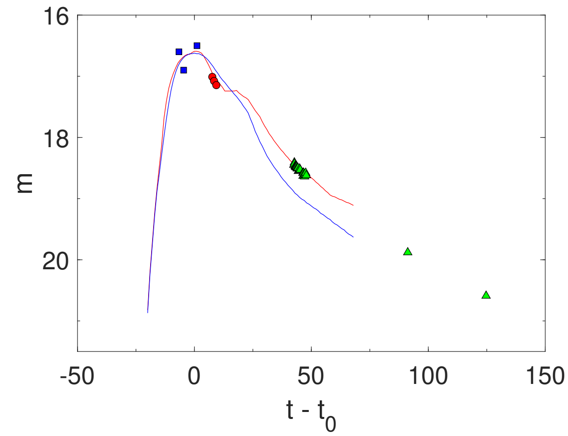

Fig. 10. AT 2017eve light curve. Template light curve for Type Ia SN in V (blue line) and R (red line) filters with $z = 0$ (Nugent, Kim & Perlmutter 2002), with *ASASSN* data (V filter, blue squares, Nicholls, Brimacombe & Cacella 2017), GAIA data (G filter, green triangles, `http://gsaweb.ast.cam.ac.uk/alerts/alert/Gaia17byi/`) and OAUNI data (R filter, red dots, Table 2). Time offset is $t_0 = 2457922.5$ days. The color figure can be viewed online.

m_1 data (see Table 2) in the least residual technique to obtain the value m_0 solely (see Table 5), taking into account its categorization as a Type Ia SN, the date of the peak, and the host galaxy z (see Table 1). This fitting enables us to see the *ASASSN* data dispersion around the maximum brightness date in Figure 10. However, *GAIA* data show a behavior different from the preceding SN, with a smaller fall rate than the template.

4.7. *SN 2023gfo*

The V-R and R-I colors for the single OAUNI multicolor photometry data (see to Table 2) of SN 2023gfo have been computed and are shown in Figure 11. Although its location on the diagnostic diagram is not precise enough to determine the observational period, it indicates that this SN may have occurred between days 34 and 42 following the maximum brightness. The telegram of its discovery (Moore et al. 2023), which highlights the fact that the ATLAS system found no evidence of this event three days earlier in the same area, despite the SN being discovered on May 19, supports this view. The type IIp SN 2004et data (Sahu 2006) and the OAUNI m_1 data (see Table 2) of four consecutive months in filter R are plotted together in Figure 12. Since SN 2004et's data have already been adjusted for its peak brightness time, it can be used as a kind of template. Thus, in order to obtain the offset vec-

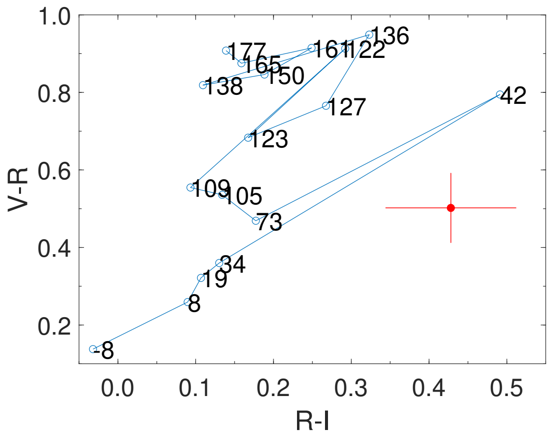

Fig. 11. $V - R$ vs. $R - I$ color diagram of a Type IIp SN with $z = 0$ (blue lines, adapted from Poznanski et al. 2002). Numbers indicate days after maximum light. OAUNI colors for SN 2023gfo using m_2 calibration are also indicated (red point). The color figure can be viewed online.

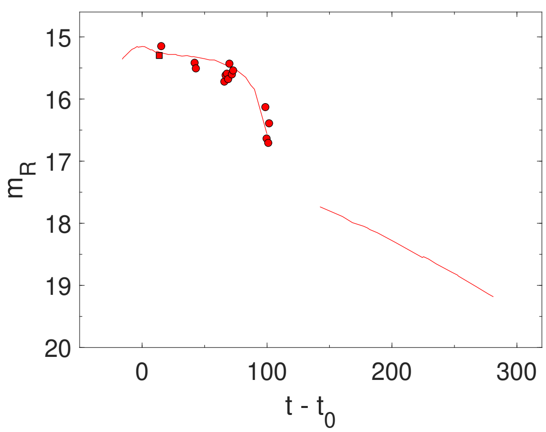

Fig. 12. SN 2023gfo light curve in the R filter. SN 2004et Type IIp light curve with $z = 0.0002$ (red squares, Sahu 2006), with OAUNI data (red dots, Table 2). Time offsets is t_0 = 2460049.7. The color figure can be viewed online.

tor (t_0; m_0), we fitted the SN 2004et light curve to a polynomial. Next, we obtained its equivalent vector (see Table 5) from the least residual approach after substituting the OAUNI m_1 data in the SN 2004et polynomial fitting. During the initial three months, OAUNI detected a 0.6 mag decline in magnitude while SN 2004et remained within the same range. In the last month, data could set SN 2023gfo at the end of the plateau phase. The OAUNI data indicate a higher fall rate compared to prior months, which is consistent with SN 2004et. Because the

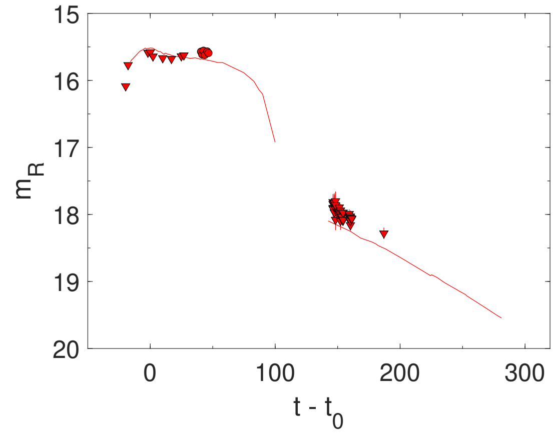

Fig. 13. SN 2023ijd light curve in the R filter. SN 2004et Type IIp light curve with $z = 0.0002$ (red squares, Sahu 2006), with ZTF data (red triangles, `https://lasair-ztf.lsst.ac.uk/objects/ZTF23aajrmfh/`), and OAUNI data (red dots, Table 2). Time offsets is t_0 = 2460088.9 days. The color figure can be viewed online.

first night of observation was on day 39 using the approach of least residual, this result supports the information provided by the diagnostic diagram.

4.8. *SN 2023ijd*

We used OAUNI m_1 data (see Table 2) and ZTF (The Zwicky Transient Facility, Bellm et al. 2016) data[12] to plot the light curve of SN 2023ijd in Figure 13. We show OAUNI and ZTF data with the SN 2004et light curve in filter R with $z = 0.0002$ (type IIp), just as for the previous SN with a similar type. We plot the SN 2004et light curve against the SN 2023ijd data following the same procedures as in the prior case. In this instance, we used ZTF data close to the peak to estimate the vector (t_0; m_0) with the least residual because the date of the maximum brightness is unknown (see Table 5). The data show a steady phase of decrease with a magnitude variation of ± 0.1 mag from +10 to +60 days following the peak. This light curve phase may represent the plateau onset phase of SN 2004et.

4.9. *SN 2023ixf*

The last SN studied was the nearest and brilliant SN2023ixf. This fact is reflected in the wide available literature data up to +225 days from AAVSO[13]. As usual, we corrected the temporal values using z

[12] `https://lasair-ztf.lsst.ac.uk/objects/ZTF23aajrmfh/`.

[13] The American Association of Variable Star Observers (AAVSO).

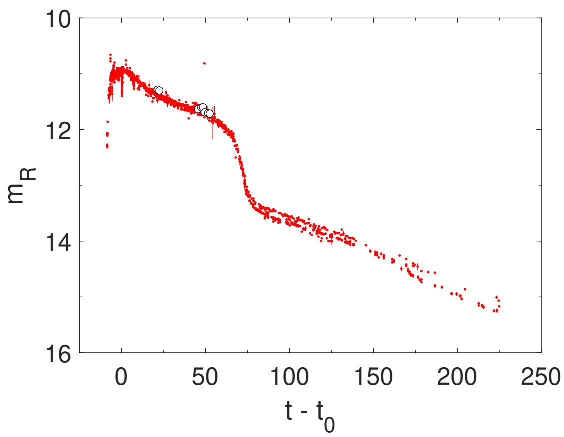

Fig. 14. SN 2023ixf light curve in R filter. AAVSO data (red points, `www.aavso.org`) and OAUNI data (white dots, Table 2). Time offset $t_0 = 2460094.0$. The color figure can be viewed online.

of its host galaxy (see Table 1), and we interpolated the peak date $t_0 = 2460094.0$ JD. This fact is supported by Filippenko, Zheng & Yang (2003), where they set $t_0 = 2460094.2$ JD. The OAUNI m_1 data (see Table 2) for the eight nights of observation of SN 2023ixf match the trend of the light curve between days +0 and +50, as can be observed in Figure 14. Following these days, the brightness shows an increase in slope, declining in 20 days from 12 mag to 13.5 mag. At last, the SN resumes its gradual decline phase.

5. CONCLUSIONS

Using the equipment available at OAUNI, the reduction of images from different SNe was accomplished effectively. These nine SNe were observed in the V, R, and I filters over a total of 43 nights, confirming the good quality of the images. This was made possible by the fact that on several observation nights, we were able to maintain an uncertainty of less than 0.09 mag despite the presence of high air masses.

Data calibration for m_1 and m_2 method was carefully examined for each filter. As a result, the agreement between both methods has an average precision of 0.096 ± 0.064. Diagnostic diagrams were used to evaluate the position of three supernovae after the maximum brightness date. The position of the supernovae found on this diagram was corroborated by different sources that recorded the date on which these events reached their peak magnitude. Through the construction of light curves using several templates and a comparison of literature and OAUNI data, we were able to study the brightness behavior of each SN. The fitting of these templates (for SNe Types Ia and IIn) and SN2004et light curve (for Type IIp) was carried out carefully using the available data close to the peak and seeking to ensure that the residual was as small as possible (> 0.001). The viability of conducting precise astronomical photometric programs at the OAUNI site is validated by this work.

The authors are grateful for economic support from Concytec (Contrato N^o PE501081907-2022-PROCIENCIA, Contrato 133-2020 Fondecyt). Special thanks to the Huancayo Observatory staff for the logistic support and to J, Tello, M. Zevallos, J. Ricra, R. Santacruz, D. Alvarado and E. Torre for their collaboration with the observations.

REFERENCES

Bellm, E. C., Kulkarni, Sh. R., Graham, M. J., et al. 2019, PASP, 131, 018002, `https://doi.org/10.1088/1538-3873/aaecbe`

Bersier, D., Smartt, S., & Yaron, O. 2016, NSCR, 650, 1

Bianciardi, G., Ciccarelli, A. M., Conzo, G., et al. 2023, TNSAN, 213, 1, `https://doi.org/10.48550/arXiv.2307.05612`

Brimacombe, J., Brown, J. S., Stanek, K. Z., et al. 2016, ATeL, 9439

Brimacombe, J., Post, R. S., Kiyota, S., et al. 2016, ATeL, 9332

Brown, J. S., Prieto, J. L., Shappee, B. J., et al. 2016, ATeL, 9445

Brown, P. J., Hosseinzadeh, G., Jha, S. W., et al. 2019, AJ, 877, 152, `https://doi.org/10.3847/1538-4357/ab1a3f`

Carlos Reyes, R., Ferrero, G., Navarro, F. A. R., & Meléndez, J. 2013, RMxAA, 49, 357

Filippenko, A. V., Zheng, W., & Yang, Y. 2003, TNSAN, 123

Foley, R. J., Hounsell, R., & Miller, J. A. et al. 2015, ATeL, 8434

Fulton, M., Nicholl, M., Smith, K. W. et al. 2023a, TNSAN, 124

Fulton, M., Srivastav, S., Nicholl, M., et al. 2023b, TNSCR, 871

Gress, O., Lipunov, V., Gorbovskoy, E., et al. 2015, ATeL, 8415

Itagaki, K. 2017, TNSTR, 647

_________. 2023, TNSTR, 1158

Jha, S. W., Camacho, Y., Dettman, K., et al. 2017, Anel, 10490

Krisciunas, K., Contreras, C., Burns, C. R., et al. 2017, AJ, 154, 211, `https://doi.org/10.3847/1538-3881/aa8df0`

Moore, T., Smith, K. W., Srivastav, S., et al. 2023, TNSAN, 92

Nicholls, B., Brimacombe, J., & Cacella, P., 2017, ATeL, 10509

Nugent, P., Kim, A., & Perlmutter, S. 2002, PASP, 114, 803, https://doi.org/10.1086/341707

Pan, Y. -C., Kilpatrick, C. D., Siebert, M. R., et al. 2016, Anel, 9333

Parker, S. 2016, TNSTR, 422

Pereyra, A., Tello, J., Meza, E., et al. 2015, arXiv151203104, https://doi.org/10.48550/arXiv.1512.03104

Perley, D. 2023, TNSCR, 1112

Perley, D. & Gal-Yam, A. 2023, TNSCR, 1164

Phillips, M. M. 1993, ApJ, 413, 105, https://doi.org/10.1086/186970

Phillips, M. M., Lira, P., Suntzeff, N. B., et al. 1999, AJ, 118, 1766, https://doi.org/10.1086/301032

Poznanski, D., Gal-Yam, A., Maoz, D., et al. 2002, PASP, 114, 833, https://doi.org/10.1086/341741

Sahu, D. K., Anupama, G. C., Srividya, S., et al. 2006, MNRAS, 372, 1315, https://doi.org/10.1111/j.1365-2966.2006.10937.x

Smith, K. W., Williams, R. D., Young, D. R., et al. 2019, RNAAS, 3, 26, https://doi.org/10.3847/2515-5172/ab020f

Stanek, K. Z. 2023, TNSTR, 1092

Theureau, G., Coudreau, N., Hallet, N., et al. 2005, A&A, 430, 373, https://doi.org/0.1051/0004-6361:20047152

Uddin, S., Mould, J., Zhang, J. -J., et al. 2017, ATeL, 10517

Zacharias, N., Finch, C. T., Girard, T. M., et al. 2013, AJ, 145, 44, https://doi.org/10.1088/0004-6256/145/2/44

M. Espinoza and A. Pereyra: National University of Engineering, Lima, Perú.
A. Pereyra: Geophysical Institute of Perú, Astronomy Area, Lima, Perú.